



Flow exchange, energy losses and pollutant transport in a surcharging manhole linked to street profiles

Matteo Rubinato^{a,b,*}, Louis Helms^a, Matthew Vanderlinden^a, James Hart^a, Ricardo Martins^{c,d}

^a School of Energy, Construction and Environment & Centre for Agroecology, Water and Resilience, Coventry University, Coventry CV1 5FB, UK

^b IKT-Institute for Underground Infrastructure, Exterbruch 1, Gelsenkirchen, Germany

^c Departamento de Engenharia Civil, Escola Superior de Tecnologia e Gestão, Instituto Politécnico de Leiria, Leiria, Portugal

^d Earth Surface Process Team, Centre for Environmental and Marine Studies (CESAM), University of Aveiro, Aveiro, Portugal

ARTICLE INFO

This manuscript was handled by Corrado Corradini, Editor-in-Chief, with the assistance of Dongmei Han, Associate Editor

Keywords:

Sewer/Surface flow interactions
Urban flooding
Drainage systems
Head losses
Pollutant transport
Flow exchange

ABSTRACT

Due to the increased frequency and magnitude of urban flooding events, there is a pressing need to improve the accuracy of numerical tools to better assess the hydraulic performance of new drainage systems. Nowadays, such models are inherently challenging to verify due to the difficulty of acquiring reliable data during the flood event, meaning that most models are calibrated using only an estimated measure of the extent of flooding. To address this gap, this study investigated flooding scenarios using an experimental scale facility of an urban street and manhole network, delivering a novel data-set in terms of the scale of the facility used. Several hydraulic conditions are investigated within a variety of street configurations incorporating parking slots, cars on the road and various locations of the manhole within the street. This enabled the quantification of flow exchange during hypothetical flood events for multiple cases, as well as the characterisation of energy losses, a crucial parameter that is often a source of uncertainty within numerical modelling tools. Furthermore, the experimental system was equipped with an injection system to replicate the transport of pollutants during flooding events, and this enabled the estimation of the exchange of soluble pollutants between the minor and major systems for each flooding scenario. Results obtained have confirmed the applicability of the orifice equation for the estimation of flow exchange between the two systems, showing that i) the discharge coefficients obtained (0.126–0.138) decrease as the width of the street/channel becomes narrower, ii) the surface energy loss coefficient was unaffected by all street configurations tested, iii) all tested geometries displayed significant pollutant exchange from the sewer to the street, in the range of 28–39%, demonstrating that situating the manhole closer to the edge of the street increased the mass of pollutants being exchanged to the surface and the presence of parking spaces alone did not appear to affect the mass of pollutant exchanged. These results have provided a novel series of datasets (including flowrates, flow exchange, energy losses and discharge coefficients) that could be used to calibrate and validate numerical models and be utilised as a benchmark.

1. Introduction

Flooding events in urban areas are known to have hugely detrimental effects on society by the resultant damage to infrastructure and properties, as well as posing a threat to the wellbeing of the people residing in the area (Chang, 2016; Hou et al., 2019). Global warming has led to deviations from the earth's natural hydrological cycle, as it has caused widespread melting of the earth's icecaps and increased the water vapour content in the atmosphere. The rise in temperature has led to changes in precipitation patterns, resulting in more intense rainfall

which has increased the occurrence of flooding (Bates et al. 2008; Rubinato et al., 2019; Ostad-Ali-Askari et al., 2019). For example, it is predicted that there will be a 2–28% rise in the UK's winter precipitation by 2050 (Arnell et al. 2015).

Furthermore, the process of urbanisation makes new developments increasingly susceptible to flooding (Zevenbergen et al. 2008; Rubinato et al., 2020a) due to the increasing number of impermeable surfaces (Swan 2010) and as population growth continues, the number of people at risk from urban flooding will only rise, with an increase of 900,000 more people expected to be at risk in the UK by 2050 (Houston et al.

* Corresponding author at: School of Energy, Construction and Environment & Centre for Agroecology, Water and Resilience, Coventry University, Coventry CV1 5FB, UK.

E-mail address: matteo.rubinato@coventry.ac.uk (M. Rubinato).

<https://doi.org/10.1016/j.jhydrol.2021.127201>

Received 3 July 2021; Received in revised form 8 October 2021; Accepted 9 November 2021

Available online 14 November 2021

0022-1694/© 2021 The Authors. Published by Elsevier B.V. This is an open access article under the CC BY license (<http://creativecommons.org/licenses/by/4.0/>).

2011). To aggravate the current situation, many of the urban drainage systems used are not able to perform effectively, with the flow capacity of storm sewers being limited as they were not originally designed to accommodate for the increasing levels of flow caused by urbanisation in comparison to the times when the drainage systems were built (Ofwat 2011). This is particularly prevalent in historic cities where combined sewer systems are still in use (Aronica and Lanza 2005).

Exposure to contaminants is a risk to health that can be associated with urban floodwater, depending on the source of the water (de Man et al. 2013; Shucksmith et al., 2018). Contaminants are released into wastewater due to agricultural processes and the waste that is produced by industries and the population (Deblonde et al., 2011). This results in surface runoff and sewage overflow transporting waterborne pathogens into the surface water during flood events which is sourced from contaminants including faecal matter, both from humans and animals (Schets et al. 2008). Among these contaminants are bacteria such as *E. coli* (Marsalek and Rochfort 2010) and antibiotic resistant bacteria which are found to have adverse health effects (Kim and Aga 2007; Arnone and Perdeck Walling, 2007; Rossi et al. 2004; Blanchoud et al. 2007; Sales-Ortells et al., 2015).

Flood modelling tools are increasingly necessary for predicting possible hydraulic behaviours in the event of a flood and are essential for a variety of purposes such as sewer system re-design, damage assessment, hazard maps and real time management applications. From the data generated by flood modelling along with consideration of economic, social, and environmental factors (Gallegos et al., 2009), preventative measures can be put in place to reduce the impacts of flooding accordingly. Djordjevic et al. (2013), first introduced a dual drainage model that explained all the steps needed to assess flood hazard. To date, state-of-the-art dual drainage models couple 1D sewer network flow models to 2D floodplain models (Lee et al., 2013) using orifice and weir equations to estimate the flow exchange between the two systems as a function of relative hydraulic head in the sewer and the surface (Djordjević et al., 2005). Furthermore, geometrical features such as pipe expansion, contraction as well as hydraulic conditions, supercritical or subcritical, can alter the energy losses inside manholes, and the effect of shallow water running over streets on surcharging manholes is also yet to be fully investigated (Mignot et al., 2019; Costabile et al., 2020). Therefore, not being able to accurately represent sub/surface flow exchange as well as energy losses can be considered as a potential source of uncertainty leading to errors and inaccurate predictions. To calibrate and validate these tools, modellers rely on footage obtained from CCTV cameras during flood events, as it is not safe for operators to record the events themselves in person during a flood (Tsubaki, Fujita and Tsutsumi 2010). This makes it extremely challenging to provide databases for these models, reducing the reliability of the results produced (Hammond et al. 2013). To support the calibration of numerical tools studies have been recently conducted to investigate the interactions between surface flows and sewer systems (Rubinato et al. 2013; Rubinato et al., 2017; Lee et al. 2015; Chen et al. 2016; Noh et al. 2016; Jang et al. 2018; Chang et al. 2018; Fraga et al., 2015; Gómez et al. 2013; Gómez et al. 2016; Saldarriaga et al. 2017; Gómez et al. 2013; Lopes et al. 2015; Martins et al. 2017; Rubinato et al. 2017; Beg et al., 2018; Beg et al. 2019, Rubinato et al. 2018a; Rubinato et al., 2018b; Martins et al. 2018; Kemper and Schlenkhoff 2019; Gómez et al. 2019; Tellez-Alvarez et al., 2020; Chibane et al., 2021; Golian et al., 2020). The studies available in literature have been conducted to test different flow exchange scenarios or surface flood extent, however they all replicate specific conditions, such as inlet conditions, open manholes (Lopes et al., 2015; Martins et al., 2014), or disconnected systems. Additionally, other researchers (Bazin et al., 2014) have also tested manholes in series however the scale of the model adopted and the consequent flows tested were limited to a narrow range of hydraulic conditions with Reynolds Number not always suitable for flooding conditions.

Many parameters have been found to affect energy losses in manholes, such as the depth ratio between up and down stream pipes (Hsu

et al., 1998), hydraulic conditions in different branches (Del Giudice et al., 2000), bed discordance within the manhole junction (Biron et al., 1996), the presence of external pipes linking laterally to the manhole (Ramamurthy and Zhu 1997; Zhao et al., 2006). However, energy losses in manholes during sewer to surface surcharge events have only been previously investigated within the same facility used in this study, for different hydraulic conditions and geometrical setup (Rubinato et al., 2018b). Despite all the progress made within this field, there remains a lack of validation of linking equations and a gap in the estimation of energy losses associated with surcharging manholes connected with various street profiles (Bruwier et al., 2020).

Additionally, water escaping from manholes during flooding events is often polluted and can contain sediments, which are transported across urban areas and are a source of health risk. Although the presence of contaminants such as these in surface flows is well known (Naves et al., 2020), there is still a lack of research into the extent of the exchange of pollutants during flood events between drainage networks and surface flows (Beg et al. 2020). This includes the quantification of the exchange and its spreading, despite some progress made in the field to optimise measuring techniques (Nichols and Rubinato, 2016; Rojas Arques et al., 2018). Nevertheless recent attempts have been made to include health risk assessment within urban flood models based on a prediction of wastewater concentration within surface flood waters (Mark et al., 2018). Current modelling approaches to determine how wastewater concentrations vary spatially and temporally relative to sewer surcharge events are based on the solution of the Advection Diffusion Equation (ADE). The ADE was originally developed by Taylor (1954) for turbulent pipe flow, although it is now commonly applied within a range of water quality applications including surface waters and urban drainage networks. To implement an accurate use of the 2D ADE it is fundamental to understand both the local 2D velocity fields as well as the turbulent diffusion coefficients. On top of this information, which is needed nowadays, there is a current lack of data on the flow exchange between sewer systems and urban surfaces. This is important as the risk of infection can be dependent on a pathogen's concentration in the water (Hofstra 2011). Gaining a better understanding of the potential quantities of these pollutants that are being transported into surface flows will aid in making informed decisions. These decisions can be on things such as what further measures need to be taken in sewage treatment facilities, as well as altering the designs of future sewage systems to mitigate against these risks (Mostafa et al., 2016).

The primary aim of this research is to quantify and provide a better understanding of flow exchange between sewers and urban surfaces to improve flood modelling. Nowadays it is important to demonstrate the theoretical capability of the current modelling types available via robust experimental validation, as this provides confidence in future numerical studies that investigate surface to sewer exchange flow. Therefore, we strongly believe that the results provided could be an essential source for numerical modellers across the world to be used to calibrate and validate numerical tools. Furthermore, the applicability of the orifice equation was tested for these complex configurations and the tests conducted were analysed to study the effects that the geometry of a street can have on i) the flow exchange estimation between a sewer and a hypothetical surface, ii) the energy losses inside a surcharging manhole during urban flooding events and iii) the transport of soluble pollutants between the two systems.

2. Experimental model

To address the gaps identified in various literature, an experimental campaign was conducted using a physical model, constructed and situated at the University of Sheffield (Rubinato, 2015). This model consists of a linked sewer-surface system at a scale of 1:6, as shown in Fig. 1, and has previously been used to compare InfoWorks results to experimental data (Rubinato et al., 2013) as well as to provide a better understanding of urban flooding phenomena (Beg et al. 2020; Rubinato et al. 2017;

Martins et al. 2018; Rubinato et al., 2018a,b; and Martins et al. 2017; Lopes et al., 2014; Beg et al., 2018). The model, constructed with clear acrylic (75 mm internal diameter), replicates a sewer pipe system which is connected to a hypothetical urban surface by a manhole (240 mm diameter). The surface (6.6 m long and 1.180 m wide) is also made of acrylic (Manning's $n = 0.009 \text{ sm}^{-1/3}$) and it is inclined at a slope of 0.001 m/m. At full scale, these dimensions would be an acceptable and common design for a UK urban drainage system (Defra 2011). Tests were carried out on the 5 different street profile configurations shown in Fig. 2 (and Fig. A1 in Appendix A), in order to determine how differing geometries affect the exchange of flow and pollutants between the sewer and the surface during flooding conditions.

The applicability of the orifice equation commonly used to quantify the flow exchange between the major and minor systems, along with the corresponding range of discharge coefficients under steady state flow conditions, was obtained via a series of tests that have been conducted using the experimental facility described. The inflows to the pipe were varied to generate increasing surcharge into the street via a single manhole, therefore simulating conditions where the hydraulic head in the sewer system was greater than the surface flow depth.

The flow within the system was measured using electromagnetic flow meters, which were situated at the inlets of both the surface (Q_{InF}) and the sewer (Q_{InS}), while there was another located at the sewer outlet (Q_{OutS}). Steady flows into the sewer and onto the surface were controlled using a butterfly flow control valve, which was controlled by Labview™ software along with the electromagnetic flowmeters and pressure sensors (Rubinato, 2015). The accuracy of the flowmeters has been validated using volumetric discharge readings using the laboratory measurement tank. Flows were able to be set and entered the model via both the sewer inlet and the floodplain inlet (4.30 l/s for all cases kept steady), with the flow exchange occurring within the manhole structure replicating typical flooding scenarios. To obtain temporally averaged values, the data was collected over a period of 5 min after the flow had been allowed to stabilise (5 mins, measurement rate 2 Hz).

To simulate the transport of solutes, Rhodamine WT, a neutrally buoyant fluorescent dye, was injected into the inflowing sewer pipe (Shucksmith et al., 2018). The concentration of the dye was measured by two Cyclops-7F™ fluorimeters (cyclops 1 and 2 in Fig. 1) which were located before and after the manhole, respectively. This was done to assess the solute exchange under different flow conditions for dissimilar street profiles on the hypothetical urban streets. The dye was released into the system in pulses (15 s) and was injected at a distance greater than 10D from the manhole (D being the diameter of the sewer pipe) to guarantee the full mixing of the pollutant within the water and provide an accurate measurement of its concentration before and after the manhole (Gotfredsen et al., 2020; Rutherford, 1994). For this experiment, dye of concentration 10^{-3} mg/L was fed into a constant head tank (see image below), from where injections into the sewer pipe were

controlled by a manual open/close valve. For each test conducted, the measurements were continuous and the electrical sensor output was converted into a concentration using experimentally predetermined calibration equations (Beg et al., 2020).

Pressure was measured at various location within the sewer and the surface by using GEMS pressure transducers, fitted within the pipe invert and the bed of the hypothetical surface. Transducers were calibrated such that transducer output signal (mA) can be directly related to gauge pressure. This step was completed using a pointer gauge with an averaged recorded error between measured values and defined calibration relationships. P_{sewer} (accuracy $\pm 0.72 \text{ mm}$ within the water depth of 0–600 mm) and $P_{surface}$ ($\pm 0.109 \text{ mm}$ within the water depth of 0–100 mm) were located 350 mm and 460 mm respectively from the centre of the manhole (Fig. A2 in Appendix A). This equipment was calibrated so that the electrical output signal (mA) could be directly related to gauge pressure (Rubinato et al., 2017). All pressure transducers were linked to Labview software such that the readings from the facility instrumentation were logged against time.

2.1. Method for analysis of results

2.1.1. Estimation flow exchange

To determine the quantity of the flow from the sewer that reaches the surface, the mean exchange rate through the manhole was calculated as follows:

$$Q_e = Q_{InS} - Q_{OutS} \quad (1)$$

where Q_e = Mean steady state flow exchange rate through the manhole (m^3/s), Q_{InS} = Inflow of water into the sewer (m^3/s), Q_{OutS} = Outflow of water from the sewer (m^3/s). The instrument errors of the tests were calculated to determine the accuracy of the flow exchange results, providing minimum and maximum values for the flow exchange.

$$\xi_f = (Q_{InS} - Q_{OutS}) \frac{Q_e}{Q_{InS}} \quad (2)$$

where ξ_f is the instrument error (l/s).

2.1.2. Estimation of discharge coefficients

The orifice equation is the most typical approach used to quantify the flow exchange from the sewer to the surface when the total head in the sewer pipe is more than that of the surface flow (Rubinato et al., 2017). The corresponding discharge can be calculated as follows:

$$Q_e = C_i A_M (2g)^{1/2} [h_p - (h_s + Z_{crest})]^{3/2} \quad (3)$$

where Q_e = Mean steady state flow exchange rate through the manhole (m^3/s); C_i = Discharge coefficient; A_M = Manhole area (0.045 m^2); g = Acceleration due to gravity (9.81 m/s^2); h_p = Flow depth above the

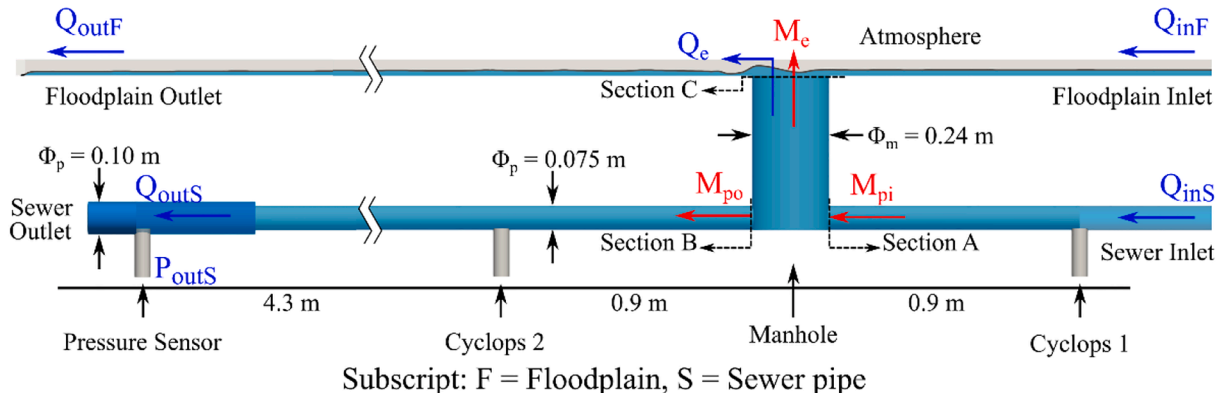


Fig. 1. Linked sewer/surface scaled experimental model (Beg et al., 2020).

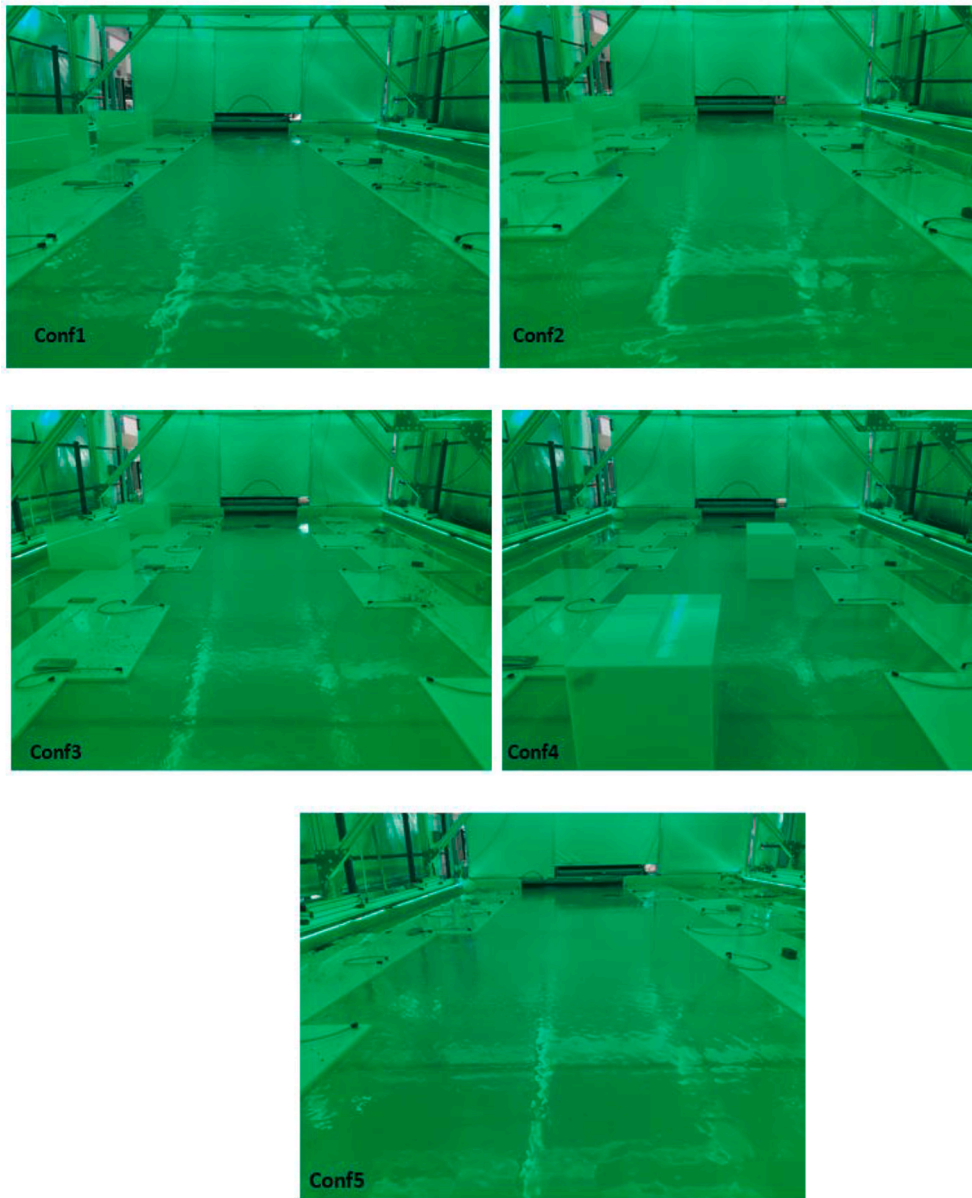


Fig. 2. View from downstream of the 5 configuration tested.

surface elevation (m); h_s = Surface elevation (m); Z_{crest} = Height difference from the invert of the pipe system to the surface level (m), respectively.

By rearranging this equation, it is possible to estimate the values of the discharge coefficients that could be used for the calibration and validation of numerical tools for the experimental scenarios tested within this study. Thus, the discharge coefficient can be calculated as follows:

$$C_i = \frac{Q_e}{A_M(2g)^{\frac{1}{2}}[h_p - (h_s + Z_{crest})]^{\frac{1}{2}}} \quad (4)$$

2.1.3. Characterisation of energy losses inside the manhole

A sewer system overflows when it has reached its maximum capacity. Therefore, there is a flow exchange between the sewers and the floodplain. According to Rubinato et al., (2018b), if the pipe inflow meets steady flow conditions, the energy balance equation over the control volume can be written as follows:

$$\rho g(H_1 Q_{ms}) = \rho g(H_3 Q_{Oms} + H_2 Q_e + \Delta H Q_{ms}) \quad (5)$$

where ρ is the density of water (kg/m^3), g is the gravitational acceleration (m/s^2), H_1 , H_2 and H_3 are the hydraulic heads of the upstream pipe flow, surface flow and downstream pipe flow, respectively (m). By rearranging Eq. (5), it is possible to describe the total energy loss during surcharged conditions inside a manhole as follows:

$$\Delta H = H_1 - (H_3 \frac{Q_3}{Q_1} + H_2 \frac{Q_e}{Q_1}) \quad (6)$$

By virtue of the pipe flow being pressurized, the hydraulics heads can be written as follows:

$$H_1 = \frac{u_1^2}{2g} + \frac{P_1}{\rho g} + z_1 \quad (7)$$

where u_1 is the mean flow velocity at the reference point 1 in the units of (m/s), $P_1/\rho g$ is the pressure head at the reference point 1 (m) and z_1 is the flow elevation above datum at each reference point (m). With both the inlet and outlet pipes pressurized and the assumption that frictional losses are negligible over the control volume (Ramamurthy et al., 1988; Pfister and Gissoni 2014; Zhao et al., 2006, Zhao et al., 2008), the

energy loss coefficients associated to the stream of flow that runs through the manhole (K_{13}), to the overflow into the urban surface (K_{12}) and the total coefficient (K_{tot}) can be describe as follows:

$$K_{13} = \frac{H_1 - H_3}{\frac{u_{ms}^2}{2g}} \tag{8}$$

$$K_{12} = \frac{H_1 - H_2}{\frac{u_{ms}^2}{2g}} \tag{9}$$

$$K_{tot} = \frac{\Delta H}{\frac{u_{ms}^2}{2g}} \tag{10}$$

2.1.4. Quantification of pollutant exchange

The amount of the fluorescent dye (replicating soluble pollutants) that left the manhole structure and entered the floodplain was measured by comparing the concentration in the sewer flow upstream of the manhole and that of the sewer pipe downstream of the manhole. The reduction in concentration of the solute between the inflow and the outflow allowed for the quantification of the amount of solute that reached the floodplain.

$$\frac{dM_m}{dt} = M_{PI}Q_{mS} - M_{PO}Q_{outs} \tag{11}$$

where $\frac{dM_m}{dt}$ = Rate of change of the solute’s mass within the manhole structure (mg/s); M_{PI} = Solute mass flow rate entering the manhole structure from the inflowing pipe (mg/s); M_{PO} = Solute mass flow rate leaving the manhole structure through the outflowing pipe (mg/s).

2.1.5. Reynolds numbers

To enable the upscaling of the flow conditions tested within the sewer system, Reynolds numbers for the pipe flows were calculated as follows.

$$R_e = \frac{uD}{\nu} \tag{12}$$

where R_e = Reynolds number; u = Velocity of fluid (m/s); D = Diameter of pipe (m); ν = Kinematic viscosity of water (m^2/s). The Reynolds values calculated were used to classify the turbulence of the pipe flow within the typical ranges: Laminar flow ($R_e < 2000$); Transitional flow ($2000 < R_e < 4000$) and Turbulent flow ($4000 < R_e$).

Table 1

Experimental measured data including flow exchange Q_e (l/s), flow exchange variation (l/s), surface flow depth h_s (m), pipe network head h_p (m) and calculated non-dimensional parameters inclusive of surface Froude number $Fr_{surface}$, scaled flow depth h_s/DM , Reynolds number in both pipe Re_{pipe} and manhole $Re_{manhole}$ obtained using Equation (12).

Surface Geometry	Q_3 sewer inlet (l/s)	Q_4 sewer outlet (l/s)	Q_e (flow exchange l/s)	Flow exchange variation ξ_f (l/s)	Surface flow depth h_s (m)	Pipe network head h_p (m)	Surface Froude number (/)	Scaled flow depth h_s/D_m (m)	Pipe Reynolds number Re_{sewer} (/)	Manhole Reynolds number $Re_{manhole}$ (/)
1. Rectangular Street	8.49	6.04	2.46	5.302E-05	0.0236	0.540	0.322	0.098	144,198	13,029
	9.28	6.24	3.04	6.796E-05	0.0256	0.549	0.285	0.107	157,545	16,149
	9.83	6.61	3.22	9.038E-05	0.0263	0.555	0.274	0.110	166,915	17,087
2. Parking on one side	8.50	6.07	2.43	4.956E-05	0.0221	0.539	0.356	0.092	144,247	12,879
	9.28	6.48	2.80	4.700E-05	0.0230	0.547	0.334	0.096	157,553	14,875
	9.82	6.57	3.24	6.605E-04	0.0244	0.554	0.307	0.102	166,632	17,193
3. Parking on both sides	8.52	6.03	2.49	4.862E-05	0.0225	0.539	0.275	0.094	144,646	13,233
	9.27	6.30	2.97	1.155E-04	0.0237	0.548	0.254	0.099	157,291	15,740
	9.79	6.56	3.23	7.220E-05	0.0244	0.554	0.244	0.102	166,276	17,157
4. Cars and parking on both sides	8.47	6.11	2.36	5.073E-05	0.0283	0.543	0.195	0.118	143,802	12,544
	9.23	6.21	3.02	1.076E-04	0.0296	0.552	0.182	0.123	156,749	16,022
	9.77	6.52	3.25	9.081E-05	0.0299	0.558	0.179	0.125	165,819	17,229
5. Parking both sides/ manhole on one side	8.52	6.05	2.43	5.488E-05	0.0204	0.535	0.328	0.085	144,560	12,868
	9.29	6.44	2.86	5.745E-05	0.0215	0.544	0.304	0.089	157,792	15,151
	9.82	6.44	3.38	1.104E-04	0.0225	0.552	0.282	0.094	166,685	17,947

2.1.6. Froude number

Similarly, Froude numbers for the surface flows were estimated to determine whether the flow on the hypothetical streets were sub-critical or super-critical at different locations along the surface. To do this, the following equation was used.

$$F_r = \frac{u}{\sqrt{gy}} \tag{13}$$

where F_r = Froude number (/); u = Velocity of flow (m/s); g = acceleration due to gravity ($9.81 m/s^2$); y = flow depth (m). Based on the Froude numbers the surface flow could be classified as either sub-critical ($F_r < 1$) or supercritical ($F_r > 1$).

3. Results and discussion

This section presents the measured flow exchange and hydraulic head values for each test conducted within the experimental facility.

3.1. Calibration of linking equations

The hydraulic conditions are displayed in Table 1 and to enable the up-scaling of the results obtained (Rubinato et al., 2020b), a series of non-dimensional parameters (Re_{sewer} , $Re_{manhole}$, $Fr_{surface}$) are included. The calculated instrument error margins in Table 1 show minimal potential error in the flow exchange values, confirming the accuracy of the physical model and the equipment used.

The maximum inflow rate for the surface (Q_1) was ≈ 4.50 l/s, while for the sewer (Q_3) system it was ≈ 10 (l/s). Based on a geometrical scale of 1 to 6, this flow rate for the sewer system corresponds to approximately 65 (l/s) in a full scale pipe system based on Reynolds similitude (0.45 m the diameter of the real site manhole). The velocities on the surface were quantified to be between 0.09 and 0.17 (m/s) for the tests reported here, with flow depths between 20 mm and 30 mm. The surface flow Froude numbers were in the range 0.179–0.356, and were hence sub-critical. Based on the Froude numbers’ similitude, this corresponds to a real scaled velocity range of 0.225 and 0.425 (m/s) in urban areas. These values are within the range that might be expected for a shallow water running over an urban surface during a flood event, and is similar to the range used by (Djordjevic et al. 2013) for the physical modelling of gully performance during flood events.

Table 2 shows the calculated mean discharge coefficients C_i for each of the surface configurations tested and the 3 different overflow

Table 2
 Q_e error margins and correlation.

Surface Geometry	Q _{e,min} (m ³ /s)	Q _{ex} (m ³ /s)	Q _{e,max} (m ³ /s)	C _i	Trendline equation	R ² value
Conf. 1. Rectangular Street	0.002403	0.002456	0.002509	0.063	y = 0.3825x - 0.0026	0.9122
	0.002976	0.003044	0.003112	0.071		
	0.003130	0.003221	0.003311	0.071		
Conf. 2. Parking on one side	0.002378	0.002428	0.002477	0.062	y = 0.4066x - 0.0031	0.9981
	0.002757	0.002804	0.002851	0.065		
	0.003175	0.003241	0.003307	0.071		
Conf. 3. Parking on both sides	0.002446	0.002494	0.002543	0.063	y = 0.3699x - 0.0025	0.9749
	0.002851	0.002967	0.003083	0.069		
	0.003162	0.003234	0.003306	0.071		
Conf. 4. Cars and parking on both sides	0.002314	0.002365	0.002415	0.062	y = 0.4415x - 0.0035	0.9274
	0.002912	0.00302	0.003128	0.071		
	0.003157	0.003248	0.003338	0.072		
Conf. 5. Parking both sides/ manhole on one side	0.002371	0.002426	0.002408	0.063	y = 0.4787x - 0.0041	0.9966
	0.002798	0.002856	0.002913	0.067		
	0.003273	0.003383	0.003493	0.074		

conditions. The results show that as the sewer inflow increases, the rate of flow exchange becomes greater for all 5 street geometries. The greatest rate of flow exchange change was recorded when the manhole was situated closer to the side of the road at the highest sewer inflow.

Fig. 3 displays relationships between flow exchange Q_e and the orifice equation applied, incorporating results existing in literature ((Rubinato et al. 2017) carried out using the same experimental model with a much wider and clear surface geometry, width 4 m, no street profiles replicated)..

It can also be seen that the flow exchange – orifice value relationships for each of the geometries fall within a similar range. The graph shows a clear relationship between the width of the surface flow channel and the orifice value. The linear regression lines of both sets of data have similar gradients, while the results from Rubinato et al. (2017) have dissimilar orifice values within the same range of flow exchange. The strength in the correlation of these values suggests that the linear regression model can be used to estimate the flow conditions for similar geometries.

The resultant discharge coefficients from Rubinato et al. (2017) were in the range of 0.160–0.174, while for a similar range of flow exchange

used in this study, the range found in these tests is 0.126–0.138. Despite this, the gradient of the linear regression model for the previous study is very similar to those derived from this experiment, showing there is a clear relationship between the width of the surface and the resulting discharge coefficient considering the differences estimated. As the width of the channel decreases, the corresponding discharge coefficient decreases.

As shown in the discharge coefficient and orifice value section, the flow exchange rate Q_e and the orifice value for each configuration show a linear relationship as the flow rate increases, with the same trend being shown in the previous study by Rubinato et al. (2017) using a wider channel width (4 m instead of 1.180 m). Each of the linear regression models having an R² value greater than 0.96 also supports the accuracy of the trendlines created. This pattern suggests that the linear trendline equations, for example the ones presented in Table 3, for different street geometries, could potentially be used to predict the flow exchange from the sewers based on the orifice value that is observed. Further testing at a wider range of flow exchange values would be required to confirm whether the relationship remains linear as the values increase/decrease. Although, the linear pattern shown by the results of Rubinato et al. (2017) across a much wider Q_e range indicates that the geometries from this study would likely show the same behaviours.

Although each of the trendlines are specific to the individual configurations, all 5 of the equations found in this study show very similar gradients and close x-axis intercept values. This indicates that the relationships shown in this study can be used to estimate the flow exchange of different street types of similar width, given that they have the same

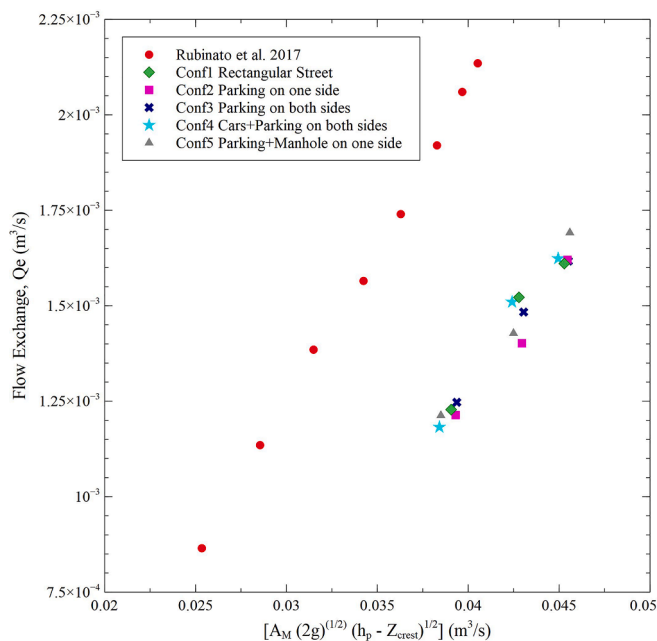


Fig. 3. Q_e vs Orifice equation to determine C_i (compared to previous studies Rubinato et al., 2017).

Table 3
 Q_e and orifice value correlation.

Surface Geometry	Q _e (m ³ /s)	Orifice Value (m ³ /s)	Trendline equation	R ² value
Conf. 1. Rectangular Street	0.002456	0.039062	y = 0.1256x - 0.0024	0.9656
	0.003044	0.042792		
	0.003221	0.045286		
Conf. 2. Parking on one side	0.002428	0.039309	y = 0.1301x - 0.0027	0.9778
	0.002804	0.042955		
	0.003241	0.045461		
Conf. 3. Parking on both sides	0.002494	0.039372	y = 0.1211x - 0.0023	0.9980
	0.002967	0.043050		
	0.003234	0.045511		
Conf. 4. Cars and parking on both sides	0.002365	0.038416	y = 0.1377x - 0.0029	0.9793
	0.00302	0.042413		
	0.003248	0.044950		
Conf. 5. Parking both sides/ manhole on one side	0.002426	0.038497	y = 0.1337x - 0.0028	0.9829
	0.002856	0.042493		
	0.003383	0.045591		

sewer and manhole dimensions. To do the same for streets with other sewer arrangements, further experimentation such as this study, would need to be carried out using physical models of these alternative sewer systems. It would also be beneficial to do this so that the magnitude of the effects caused by the sewer arrangement can be compared too.

3.1.1. Variations in surface velocity

At the position P_{surface} upstream of the manhole, the Froude numbers of each geometry showed less variability and were all subcritical. Although, the values obtained for geometry 4 were noticeably lower within the range of 0.179–0.195, while the other geometries showed similar numbers between 0.244 and 0.356. The cause of this is the velocity of the surface flow, which is greatly reduced in comparison to configurations 1–3 in particular.

The velocity was calculated downstream of the manhole once the overflow and the surface flow were combined to make the most accurate representation of the surface velocity downstream of the manhole. The reason for this being that the flow is restored to its normal sub-critical conditions at this point and is no longer subject to the effects of the surcharge which causes a hydraulic jump in the region surrounding the manhole. From the results obtained, it can be noted that the presence of parking spaces, cars on the road, and the position of the manhole all have an effect in reducing the surface flow velocity. The effects of parking spaces are demonstrated by the reduction of velocity from the rectangular street which was 0.204–0.209 m/s, to the range of 0.181–0.193 m/s for both geometries 2 and 3. As the velocities are in the same range whether there is parking on one side or both sides of the street, it suggests that this has minimal effect on the surface flow.

The presence of cars on the street appears to have the greatest effect on the velocity, as there is a significant reduction to 0.134–0.146 m/s between configurations 3 and 4, which had identical parking slots. A

reason for this could be the position of the manhole, as it was positioned at the centre of the street for configuration 4. Consequently, the cars were located closer to the centreline of the manhole (where measurement points were situated) than the parking slots were, having greater influence on the measurements.

When the manhole was positioned near the side of the street there was also an observed velocity reduction to the range of 0.15–0.161 m/s, although it was not as great of an increase as the one seen for geometry 4. As the number and size of the parking slots on either side was altered from that of configuration 4, they could have caused additional affects to the velocity. However, to determine if this was true and to confirm that cars being present on the street has a greater effect on the velocity, additional tests would be required. This could be done by placing the manhole on one side with identical parking arrangements to directly compare them, or to assess different sizes, numbers and arrangements of parking slots when the manhole is central to first identify how strong their influence is.

The Froude numbers calculated downstream from the manhole along the surface show that the most significant difference between the Froude numbers of each geometry occurs at the position that is 510 mm from the centre point of the manhole. At this position, the Froude numbers for geometries 1–4 are supercritical whereas geometry 5 provides sub-critical values. This shows a clear influence from the position of the manhole on the criticality of the surface flow, likely due to the interaction between the flow in proximity of the surcharging manhole with the curb of the model.

3.2. Characterisation of energy losses

Fig. 4 displays the experimentally determined hydraulic heads losses (H_1-H_3) , (H_1-H_2) and ΔH plotted against sewer inflow velocity head

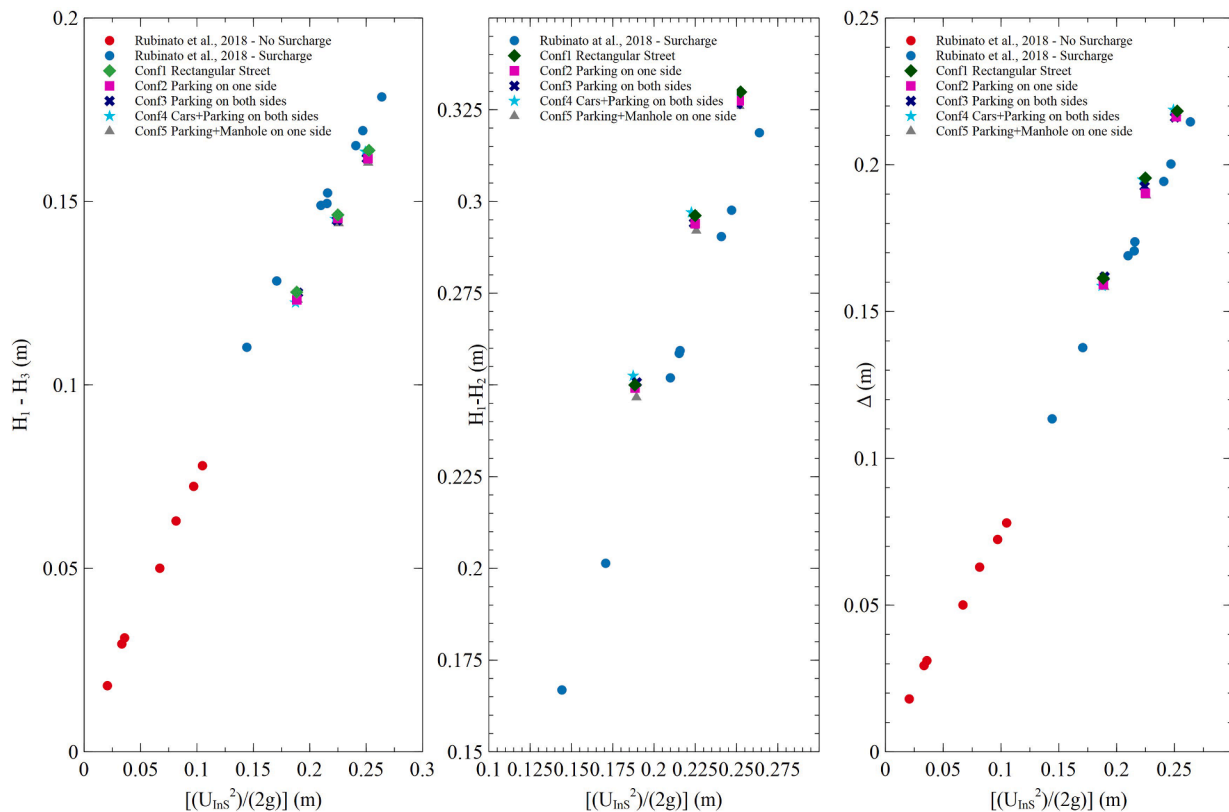


Fig. 4. Experimentally determined hydraulic head losses ΔH_{13} , ΔH_{12} , ΔH against velocity head components calculated.

Table 4
Energy loss coefficients calculated for each test.

Surface Geometry	K_{13}	K_{12}	K_{Tot}
Conf. 1. Rectangular Street	0.653 ($R^2 = 0.991$)	1.315 ($R^2 = 0.997$)	0.864 ($R^2 = 0.998$)
Conf. 2. Parking on one side	0.646 ($R^2 = 0.996$)	1.308 ($R^2 = 0.997$)	0.815 ($R^2 = 0.995$)
Conf. 3. Parking on both sides	0.649 ($R^2 = 0.991$)	1.311 ($R^2 = 0.997$)	0.859 ($R^2 = 0.998$)
Conf. 4. Cars and parking on both sides	0.654 ($R^2 = 0.999$)	1.332 ($R^2 = 0.995$)	0.869 ($R^2 = 0.987$)
Conf. 5. Parking both sides/ manhole on one side	0.641 ($R^2 = 0.994$)	1.296 ($R^2 = 0.999$)	0.849 ($R^2 = 0.986$)

($u_1^2/2g$) components for the tests conducted in surcharging conditions. It is possible to observe a clear linear relationship between head loss and velocity head of the sewer inflow. By considering the slope of the regression lines fitted to the experimental data, head loss coefficients (K) were determined. These coefficients and their confidence limits ($R^2 > 0.986$ for all the cases) are given in Table 4.

The results obtained are in line with what is available in literature (Rubinato et al., 2018a,b), confirming that for all the cases, the energy loss coefficient linked with the flow exchange (K_{12}) is higher than the energy loss coefficient associated with the flow through the sewer (K_{13}) demonstrating that higher energy losses are generated inside the manhole during surcharging conditions.

Furthermore, it is important to highlight that the trends observed are very similar for all the configurations tested. This means that parking slots and the presence of cars are actually providing a negligible effect on the energy losses linked with the overflow inside the manhole. However, it is essential to note that the configuration which creates the more substantial change is configuration 5, with parking on both sides and the manhole on one side, where K_{12} was calculated to be 1.296 (minimum value obtained).

3.3. Quantification of pollutant exchange

For each of the 5 geometries, 6–7 tests took place at 3 different rates of flow exchange. The number, length, and time of pollutant injections varied to investigate the effects this had on the percentage of the pollutant that is exchanged to the surface.

Tables 5–9 in Appendix B present the percentage of the pollutant entering the sewer inflow pipe that was exchanged to the surface flow on each of the surface geometries at varying flow exchange rates. The data is summarised in Fig. 5.

With exception to the rectangular street geometry, all the other configurations show a linear increase in the percentage of the pollutant exchanged as the flow exchange becomes larger, but it is also important to acknowledge that for cars/parking on one side, parking on one side and parking/manhole on one side there may be a possibility of an exponential trend. This requires verification, needing higher concentrations of pollutant to be injected and additional hydraulic conditions to be tested. The exchange values for configuration 5 and the percentage pollutant exchanged at the highest flow exchange rate for configuration 4 are significantly larger than the results shown from the other tests, indicating that there is a link between the presence of obstructions around the manhole and the quantity of pollutant that is exchanged. The variations in the number, time and length of the pollutant injection pulses did not appear to affect the percentage of pollutant present in the sewer that was transported to the surface, as there are no distinct variations between the percentages calculated under different pulse conditions. This is likely due to the flow conditions being steady state, meaning there were no variations in the flow conditions between pulse injections.

The pollutant exchange results show that for all the surface geometries a relatively large proportion of the pollutant mass was transported

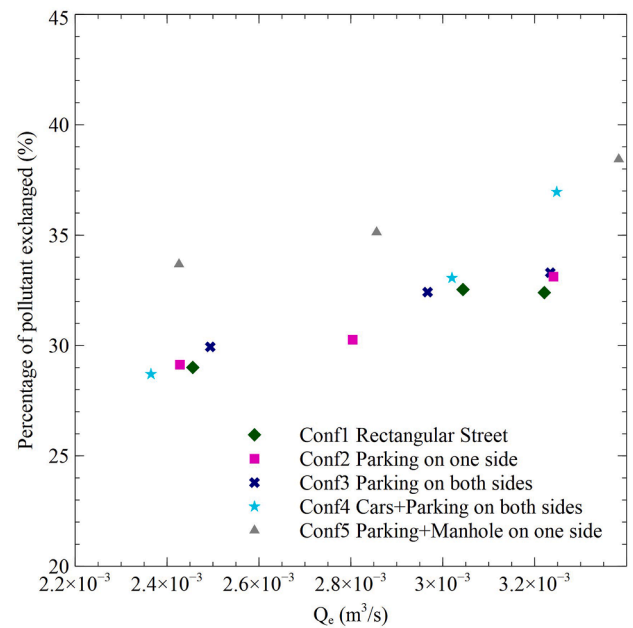


Fig. 5. Q_e vs Average pollutant exchange %.

to the surface (28–39% - Fig. 5). Being able to quantify the percentage of pollutant reaching the surface is an important step in assessing the level of risk associated with the concentration of individual pollutants present in real sewer systems. Using data such as this, samples can be taken of a sewer's effluent for testing so to measure the concentration of the pollutants found in the samples. Combining the pollutant concentrations, the percentage of the pollutant discharge and the flow exchange data, the mass of individual pollutants reaching the surface can be estimated so that their levels can be monitored as to whether they exceed acceptable levels. Doing so will help indicate whether actions need to be taken to treat the contamination.

The results of the various soluble pollutant tests identify that a significantly greater percentage of the pollutant was exchanged to the surface when the manhole was located closer to the edge of the model street. One reason for this could be due to the decreased surface velocity compared to configurations 1–3 where there similarly are not any obstructions on the road. The likely cause of the decreased flow velocity is the frictional forces acting on the water at the edge of the channel, which for configuration 5 is far closer to the centreline of the manhole where the velocity was measured. Another noticeable value in the results is that the percentage of pollutant exchanged increased largely for configuration 4 when the flow exchange value reached $0.003248 m^3/s$. A possible reason for this is the presence of cars on the street. However, this theory is not supported when the flow exchange for configuration 4 is lower, as it produced similar percentages of the pollutant being exchanged as geometries 1–3 within that flow range.

The key difference shown is the substantial decrease in surface velocity for geometries 4 and 5 which are within the range of 0.134–0.161 m/s, from those shown for geometries 1–3 between 0.181 and 0.209 m/s. The decrease in surface velocity could allow more flow exchange between surface and manhole, creating hydraulic conditions that could lead to an expansion of the hydraulic jump region when the flow exits the manhole and passes from subcritical to supercritical.

Geometries 2–5 all show a continuing increase in pollutant exchange as the flow exchange rate increases. The rectangular street is the one exception to this, as when Q_e increases from 0.003044 to 0.003221 m^3/s , the percentage of pollutant exchanged decreases from 32.54 to 32.40%. Although this is not a large decrease, it is a deviation from the patterns shown by other surface arrangements which is noteworthy. The key difference in the results for geometry 1 is that its surface velocity is by far the highest. However, there is a slight decrease in velocity between the 2 highest exchange rates corresponding with the pollutant exchange decrease. To determine whether the rectangular street would continue to deviate from the patterns displayed by the other geometries, further tests at higher flow exchange rates would need to be carried out.

Additionally, the flows observed in the sewer pipes and manhole during the experimental tests showed high turbulence, meaning that the movement of particles within the flow was very erratic. The turbulence shown in the sewer network is likely a contributing factor to the slight variation in pollutant exchange percentages between tests carried out at the same inflow and pollutant injection times/numbers, despite the flow conditions being similar. The random nature of the particle movement could have affected the quantity of the pollutant that left the pipe flow and entered the manhole. The same principal can be applied within the manhole structure, as the turbulence may have affected the quantity that was discharged to the surface and the quantity retained in the manhole that later re-entered the sewer. The effect of the turbulence would have been lesser in the manhole, as the Reynolds numbers for the manhole were much lower than those of the sewer pipes.

Finally, the similarities in the percentages exchanged for geometries 1–3 suggest that the presence of parking spaces had no noticeable effect on pollutant exchange to the surface when the manhole was positioned at the centre of the street. This is despite the parking spaces causing a reduction in the surface flow velocity.

3.4. Limitations and suggested future research

3.4.1. Unsteady flow states

All tests analysed in this study were carried out under steady state flow conditions, meaning the flow rates entering the sewer and the manhole remained constant. These are idealised conditions, as in reality it is unlikely that the flow in the sewer, or on the surface for that matter, will remain constant due to variance in factors such as rain intensity and sudden surges of water into the system. The use of steady conditions is beneficial for observing the effects of the surface geometry more clearly, both regarding flow exchange and pollutant exchange, as there are fewer contributing variables. Now that the preliminary effects of the manhole location, parking slots and presence of cars are known, unsteady state conditions will be implemented to better imitate real scenarios that would occur in the event of a flood. Moreover, the transport of pollutants in-between the surface and sewer systems are particularly affected by the surrounding soil and aquifer strata. Ignoring the effects of aquifers and other urban underground infrastructure partly explains the linear increasing trend of pollutant exchange and the hypothetical exchange rate of 28–39%. Therefore, the experimental model will be adjusted to account for the complex nature of dynamic hydraulic processes among surface - subsurface - urban infrastructure - hydrogeology - groundwater

systems.

These steady state flow conditions explain why consistent percentages of the pollutant were exchanged to the surface despite the number and length of solute impulses changing. If the same tests were undergone using unsteady conditions, it would be expected that the solute exchange percentages would be more varied. This would be most apparent when the pollutant injection patterns vary, but would even be observed under identical injection quantities, lengths, and times between tests as there is no guarantee that the flow conditions will be the same upon the point of injection. Unsteady flow hydrographs based on real rainfall events could be downscaled and simulated within the experimental facility for a more complex scenario (Rubinato 2015).

3.4.2. Effects of manhole covers

Another characteristic of typical streets which was not included in this study was the presence of manhole covers, assumed to have been removed during the worst case scenario of being lifted due to the flooding of the manhole itself. The effects of different manhole covers on flow exchange into the sewer system from the surface (without water entering the sewer inflow pipe) and the surface velocity in the vicinity of the manhole has been investigated using the same physical model as this study by Martins et al. (2018). A similar method to this could be applied to the model with the manhole surcharging to investigate how the covers may influence the flow exchange to the surface and the percentage of the pollutant which is discharged in comparison to this study, linking the velocity profiles within the quantity of flow exchange (Kesserwani et al., 2015). Furthermore, having completed these initial tests and gained information regarding the influence of street profiles, more complex scenarios involving manholes in series/parallel should be considered for a more realistic replication of storm catchment basins.

3.4.3. Location of the manhole, roughness and slopes

Within this experimental campaign, the manhole was located at two different positions. However, it is essential to conduct further studies to verify the impact that various locations may have on the flow exchange between sewers and urban surfaces. This is significant because different countries have dissimilar guidelines, and sometimes environmental constraints determine the specific locations of the manholes. Furthermore, manholes in series as previously mentioned could produce novel sets of data which could increase the complexity of this experimental model and test even further the performance of numerical models in assessing and predicting flow exchange between minor and major systems. Future work should investigate the effects of different lid and cover designs on the scale and nature of flow exchange, surface to sewer interaction flows during super-critical surface flows and/or very low flow depths as well as the behaviours shown under more complex two phase air/water flows which have not been investigated by the tests conducted here.

Finally, for this study the roughness used was $0.009 \text{ sm}^{-1/3}$, however, different values may have implications for relative head calculations at these interaction nodes. Future studies will include different rough surfaces that will be created from sand paper, perforated sheet and woven wire mesh.

3.4.4. Limitations with availability of comparable data

Whilst this was a driving factor in undergoing this study due to the necessity of obtaining data, it is also a hinderance to the validity of the findings.

Though there is nothing to suggest that the results presented in this report are not an accurate representation of real flooding scenarios, it is beneficial to be able to compare the results to similar studies so that

comparisons can be made and inspiration for further research can be taken to broaden the available spectrum of knowledge.

As previously mentioned in this paper, there is currently a scarcity of data within the field of quantifying flow exchange and solute exchange from sewer to surface during flooding events in urban areas. One of the principal purposes of this study was to provide a better understanding of these situations, delivering novel experimental datasets to be used for calibration and validation of numerical models. By enhancing the accuracy of existing and new numerical models, it will then be possible to inform local authorities to select design decisions for streets and sewer systems to minimise the risk of water (and associated pollutant) discharge when flooding occurs. The results show that both the highest observed flow exchange and pollutant exchange rate occurred when the manhole was placed towards one side of the street. If designs were to be purely based on these values, then it would indicate that the sewer and manhole systems should be constructed at the centre of the street. Yet, this would not take into consideration the practicality of the manhole location regarding factors such as the disruptions that would be caused by maintenance. Hence, the relative parties would need to assess these different aspects when coming to a design decision.

4. Conclusions

Due to the predicted climate changes and the consequent increase in the frequency and magnitude of rainfall events, there is a strong necessity to calibrate and validate numerical tools for a more accurate assessment of the hydraulic performance of drainage systems. However, due to the paucity of field data, this study was conducted to replicate urban flooding scenarios to provide novel datasets including flow exchange between a sewer system and a hypothetical urban surface to enable the calibration and validation of numerical models, as well as a better understanding of the relationship between overflow from manholes and the interference with multiple street profiles. Clear relationships between the street geometries and their corresponding flow exchange rates and discharge coefficients have been established. The effects on energy losses, the mass of soluble pollutant exchange caused by surface geometry, and both the sewer and surface flow conditions were also determined.

After assessing the various contributing factors to the solute and flow exchange results as well as considering the different flow condition for the pipes and surface channel, the key points to be taken from this study can be summarised as follows:

- The Q_e and corresponding orifice equation values show similar positive linear relationships within the same range, confirming the validation and application of this method to estimate the flow exchange during flooding conditions (C_i identified within the range 0.126–0.138).
- Through comparison with previous studies (Rubinato et al., 2017), the discharge coefficient decreases as the width of the street/channel becomes narrower.
- Tests showed that the sewer to surface energy loss coefficient was unaffected by all street configurations tested, suggesting that it is independent of the street layout
- All tested geometries displayed significant pollutant exchange from the sewer to the street, in the range of 28–39%.
- Situating the manhole closer to the edge of the street increased the mass of pollutants being exchanged to the surface.
- The presence of parking spaces alone did not appear to affect the mass of pollutant exchanged.

The results found are significant as they have the potential to be used for calibrating existing and new numerical models. This will enable the effects of other street geometries and conditions on the flow and pollutant exchange. Doing so will be important for enhancing the currently limited ability to quantify the exchanges occurring in existing sewer systems due to flood events. The present study shows that situating the manhole closer to the edge of the street increased the transport of pollutant to the surface. Therefore, other experiments with different manhole locations as well as flow conditions (higher Froude numbers) and more complex drain outlets that may disturb the flow pattern above the outlet are necessary. Municipalities could use the outcomes of this paper to either draw some new plans for the implementation of new drainage systems, however, the full experimental data sets provided by these experiments could help to validate detailed CFD and numerical models that are used to predict future scenarios and different flooding conditions.

As more research into quantifying flow and pollutant exchange becomes available, better estimates will be made by relevant authorities as to how severe the impacts of individual flood events could have been to the environment. This would be considered in addition to the physical damage to property and infrastructure which can already be determined, giving a greater perspective of the overall impacts of flooding. Combining these two methods of assessment would aid in the decision making associated with design methods and the appropriate actions to take as a result of individual flood events.

CRedit authorship contribution statement

Matteo Rubinato: Conceptualization, Methodology, Validation, Formal analysis, Investigation, Resources, Data curation, Writing – original draft, Writing – review & editing, Software, Supervision, Visualization. **Louis Helms:** Data curation, Formal analysis, Data curation, Investigation, Writing – original draft, Writing – review & editing. **Matthew Vanderlinden:** Investigation, Formal analysis, Data curation, Writing – review & editing. **James Hart:** Writing – review & editing, Data curation. **Ricardo Martins:** Visualization.

Declaration of Competing Interest

The authors declare that they have no known competing financial interests or personal relationships that could have appeared to influence the work reported in this paper.

Acknowledgements

This research was funded by EPSRC through the grant with the reference EP/ K040405/1. The experiments were conducted by Dr Rubinato within the experimental facility he developed for his PhD in the Water Laboratory of the Civil and Structural Engineering Department of the University of Sheffield. Dr Martins acknowledges the financial support of FCT, Portugal, through the Projects ASHMOB (CENTRO-01-0145-FEDER-029351) funded by FEDER, through COMPETE2020 - POCI, and by national funds (OE), through FCT/MCTES, and to the FCT/MCTES strategic projects UIDP/50017/2020 + UIDB/50017/2020 granted to CESAM. Finally, Dr Rubinato wants to thank his dad Leonardo Rubinato and his mum Sattin Maria Grazia for their constant encouragement and support, especially during tough times.

Appendix A

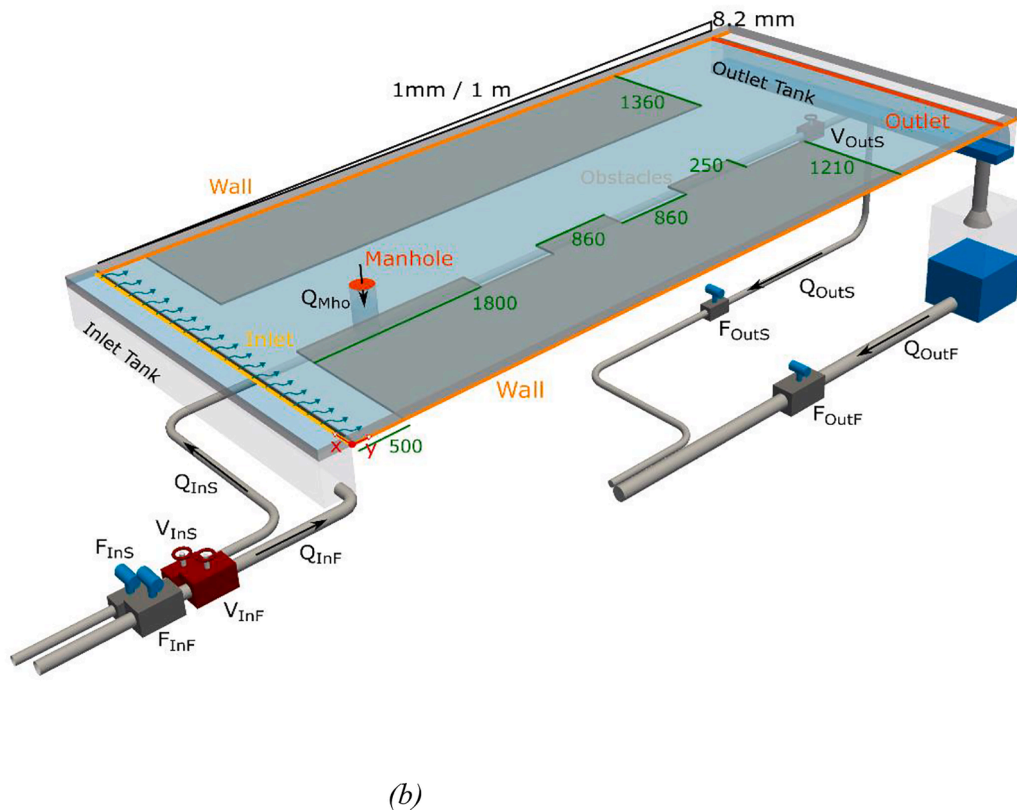
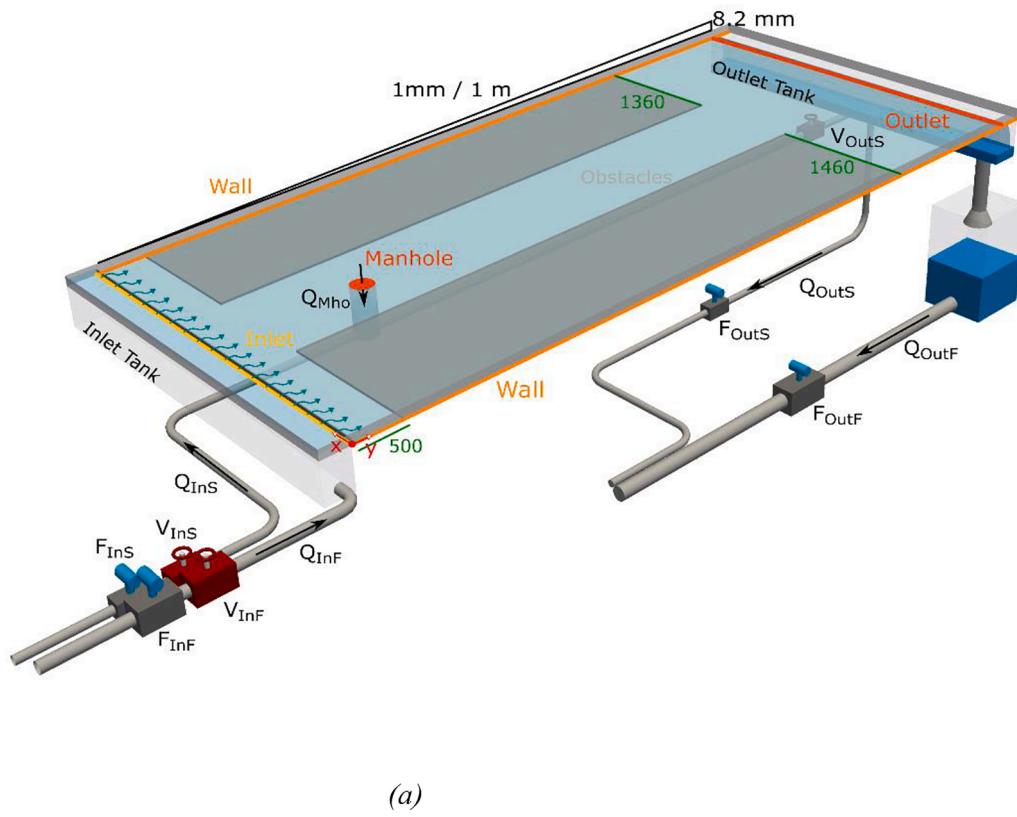
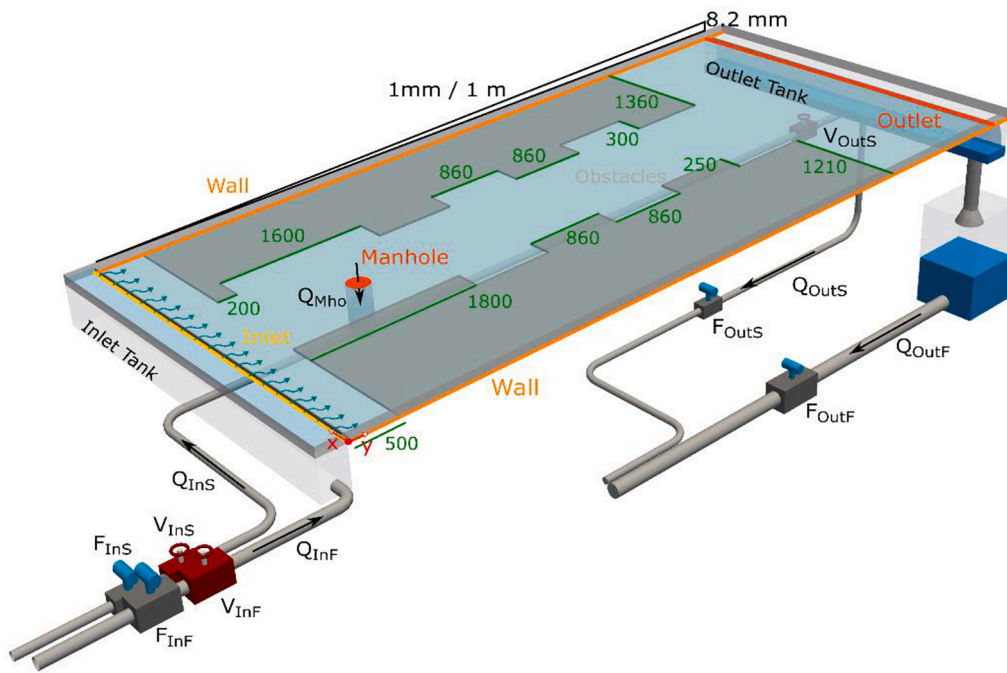
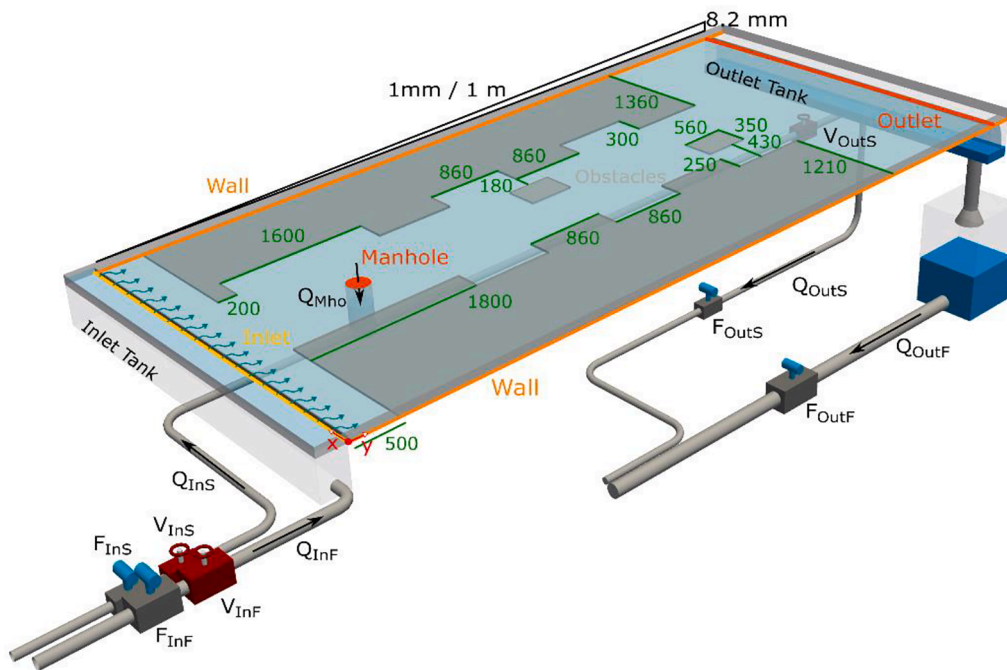


Fig. A1. The 5 configuration tested. (a) Rectangular street – Configuration 1, (b) Street with parking slots on both sides – Configuration 2; (c) Street with parking slots on one side – Configuration 3; (d) Street with cars and parking slots on both sides – Configuration 4; (e) Street with a parking slot on both sides and the manhole on one side – Configuration 5.

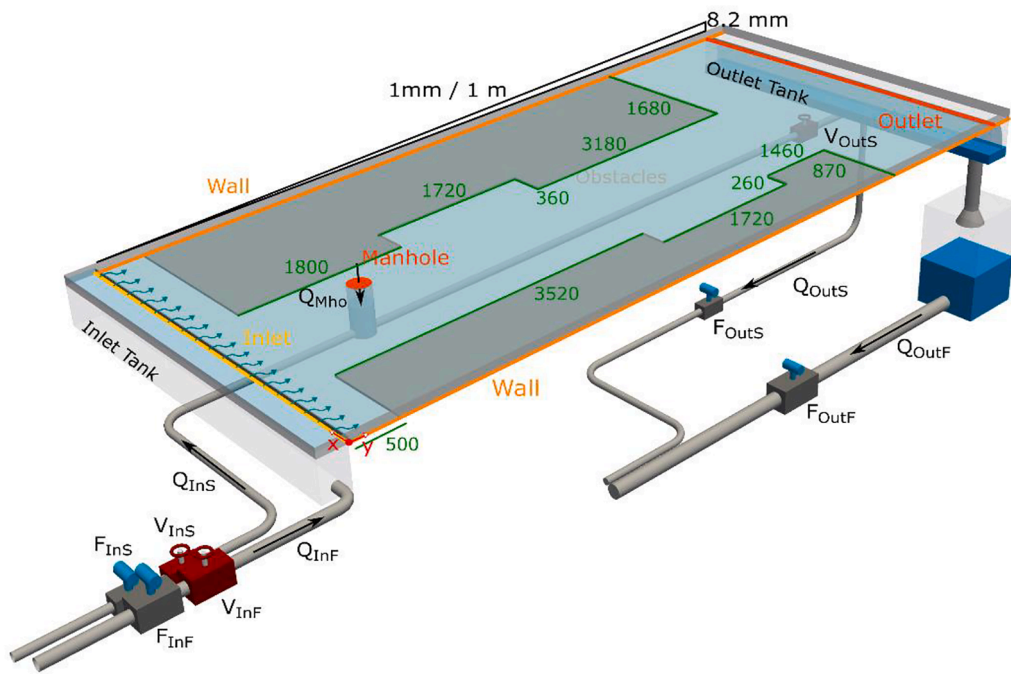


(c)



(d)

Fig. A1. (continued).



(e)

Fig. A1. (continued).

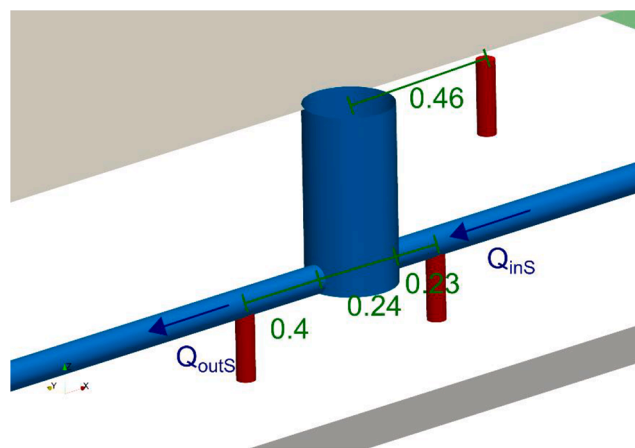


Fig. A2. Location of the pressure sensors within the sewer and the surface.

Appendix B

Table 5
Rectangular street pollutant exchange results.

Test ID	Q_e (m ³ /s)	Mass into sewer (mg/s)	Mass out of sewer (mg/s)	Mass Exchanged (mg/s)	Percentage exchanged	Average percentage exchanged
1	0.002456	0.0143	0.0101	0.0042	29.25	29.01
2		0.0131	0.0093	0.0038	29.15	
3		0.0128	0.0091	0.0037	28.95	
4		0.0267	0.0190	0.0077	28.93	
5		0.0256	0.0182	0.0074	28.95	
6		0.0268	0.0191	0.0077	28.81	
9	0.003044	0.0133	0.0090	0.0043	32.69	
10		0.0128	0.0086	0.0042	32.70	
11		0.0195	0.0132	0.0063	32.44	
12		0.0263	0.0177	0.0085	32.44	
13		0.0251	0.0170	0.0081	32.31	
14		0.0242	0.0163	0.0079	32.62	
17	0.003221	0.0137	0.0092	0.0044	32.34	32.40
18		0.0134	0.0090	0.0043	32.54	
19		0.0124	0.0084	0.0040	32.34	
20		0.0242	0.0163	0.0078	32.39	
21		0.0236	0.0160	0.0076	32.24	
22		0.0249	0.0168	0.0081	32.45	
23		0.0292	0.0197	0.0095	32.48	

Table 6
Parking on one side pollutant exchange results.

Test ID	Q_e (m ³ /s)	Mass into sewer (mg/s)	Mass out of sewer (mg/s)	Mass Exchanged (mg/s)	Percentage exchanged	Average percentage exchanged	
26	0.002428	0.0149	0.0105	0.0043	29.17	29.13	
27		0.0148	0.0106	0.0043	28.92		
28		0.0139	0.0099	0.0040	29.03		
29		0.0286	0.0203	0.0083	28.90		
30		0.0289	0.0204	0.0085	29.27		
31		0.0296	0.0209	0.0087	29.50		
32		0.0277	0.0196	0.0081	29.16		
36	0.002804	0.0136	0.0095	0.0041	30.00		30.26
37		0.0141	0.0098	0.0043	30.51		
38		0.0139	0.0097	0.0042	30.25		
39		0.0269	0.0187	0.0082	30.35		
40		0.0264	0.0184	0.0080	30.36		
41		0.0263	0.0184	0.0079	30.11		
44	0.003241	0.0136	0.0091	0.0045	33.12	33.12	
45		0.0133	0.0089	0.0044	33.07		
46		0.0128	0.0086	0.0043	33.21		
47		0.0299	0.0200	0.0099	33.11		
48		0.0255	0.0171	0.0084	32.99		
49		0.0263	0.0176	0.0087	32.97		
50		0.0252	0.0168	0.0084	33.36		

Table 7
Parking on both sides pollutant exchange results.

Test ID	Q_e (m ³ /s)	Mass into sewer (mg/s)	Mass out of sewer (mg/s)	Mass Exchanged (mg/s)	Percentage exchanged	Average percentage exchanged	
53	0.002494	0.0132	0.0092	0.0039	29.80	29.94	
54		0.0131	0.0091	0.0039	30.22		
55		0.0141	0.0099	0.0042	29.72		
56		0.0273	0.0191	0.0082	30.10		
57		0.0265	0.0186	0.0079	29.82		
58		0.0258	0.0181	0.0077	29.96		
61	0.002967	0.0137	0.0093	0.0044	32.19		32.42
62		0.0135	0.0091	0.0044	32.68		
63		0.0128	0.0087	0.0041	32.24		
64		0.0255	0.0173	0.0082	32.29		
65		0.0261	0.0175	0.0085	32.71		
66		0.0266	0.0180	0.0086	32.40		
69	0.003234	0.0138	0.0092	0.0046	33.28	33.30	
70		0.0130	0.0087	0.0044	33.39		
71		0.0134	0.0089	0.0045	33.31		
72		0.0277	0.0185	0.0092	33.14		
73		0.0263	0.0175	0.0088	33.40		
74		0.0260	0.0174	0.0087	33.28		

Table 8

Rectangular street pollutant exchange results Cars + parking on both sides pollutant exchange results.

Test ID	Q_e (m ³ /s)	Mass into sewer (mg/s)	Mass out of sewer (mg/s)	Mass Exchanged (mg/s)	Percentage exchanged	Average percentage exchanged	
77	0.002365	0.0152	0.0108	0.0044	28.87	28.70	
78		0.0153	0.0109	0.0044	28.71		
79		0.0153	0.0109	0.0044	28.79		
80		0.0311	0.0221	0.0090	28.92		
81		0.0289	0.0205	0.0083	28.90		
82		0.0278	0.0198	0.0080	28.72		
83		0.0894	0.0643	0.0251	28.03		
86	0.00302	0.0142	0.0095	0.0047	33.06		30.92
87		0.0142	0.0095	0.0047	33.00		
88		0.0139	0.0093	0.0046	32.96		
89		0.0273	0.0183	0.0090	33.12		
90		0.0272	0.0181	0.0090	33.23		
91		0.0286	0.0191	0.0095	33.26		
92		0.0838	0.0512	0.0275	32.79		
95	0.003248	0.0146	0.0097	0.0049	33.66	36.96	
96		0.0139	0.0086	0.0052	37.64		
97		0.0144	0.0090	0.0054	37.70		
98		0.0272	0.0170	0.0102	37.53		
99		0.0281	0.0175	0.0106	37.72		
100		0.0271	0.0169	0.0102	37.49		
101		0.0814	0.0512	0.0302	37.08		

Table 9

Parking + manhole on one side pollutant exchange results.

Test ID	Q_e (m ³ /s)	Mass into sewer (mg/s)	Mass out of sewer (mg/s)	Mass Exchanged (mg/s)	Percentage exchanged	Average percentage exchanged	
132	0.002426	0.0130	0.0086	0.0044	33.57	33.68	
133		0.0141	0.0093	0.0048	33.90		
134		0.0138	0.0092	0.0047	33.85		
135		0.0263	0.0174	0.0089	33.89		
136		0.0266	0.0176	0.0090	33.70		
137		0.0284	0.0188	0.0096	33.79		
138		0.0813	0.0544	0.0269	33.08		
141	0.002856	0.0133	0.0086	0.0046	35.00		35.13
142		0.0128	0.0082	0.0045	35.57		
143		0.0122	0.0080	0.0043	35.02		
144		0.0251	0.0162	0.0089	35.29		
145		0.0247	0.0160	0.0087	35.32		
146		0.0252	0.0163	0.0089	35.21		
147		0.0763	0.0500	0.0263	34.53		
150	0.003383	0.0130	0.0080	0.0050	38.62	38.44	
151		0.0128	0.0078	0.0050	38.75		
152		0.0133	0.0082	0.0051	38.14		
153		0.0252	0.0155	0.0097	38.48		
154		0.0247	0.0152	0.0095	38.58		
155		0.0248	0.0152	0.0096	38.61		
156		0.0754	0.0468	0.0286	37.91		

References

- Arnell, N.W., Halliday, S.J., Battarbee, R.W., Skeffington, R.A., Wade, A.J., 2015. The implications of climate change for the water environment in England. *Prog. Phys. Geogr.* 39 (1), 93–120.
- Arnone, R.D., Perdeck Walling, J., 2007. Waterborne pathogens in urban watersheds. *J. Water Health* 5 (1), 149–162.
- Aronica, G.T., Lanza, L.G., 2005. Drainage efficiency in urban areas: a case study. *Hydrol. Process.* 19 (5), 1105–1119.
- Bates, B.C., Kundzewicz, Z.W., Wu, S., and Palutikof, J.P. Eds., 2008. *Climate Change and Water*. Technical Paper of the Intergovernmental Panel on Climate Change. Geneva: IPCC Secretariat.
- Bazin, P.-H., Nakagawa, H., Kawaike, K., Paquier, A., Mignot, E., 2014. Modeling flow exchanges between a street and an underground drainage pipe during urban floods. *J. Hydraul. Eng.* 140 (10), 04014051.
- Beg, M.N.A., Carvalho, R.F., Tait, S., Brevis, W., Rubinato, M., Schellart, A., Leandro, J., 2018. A comparative study of manhole hydraulics using stereoscopic PIV and different RANS models. *Water Sci. Technol.* 2017, 87–98.
- Beg, M.N.A., Carvalho, R.F., Leandro, J., 2019. Effect of manhole molds and inlet alignment on the hydraulics of circular manhole at changing surcharge. *Urban Water J.* 16 (1), 33–44.
- Beg, M.d., Rubinato, M., Carvalho, R., Shucksmith, J., 2020. CFD Modelling of the transport of soluble pollutants from sewer networks to surface flows during urban flood events. *Water* 12 (9), 2514. <https://doi.org/10.3390/w12092514>.
- Biron, P., Best, J.L., Roy, A.G., 1996. Effects of bed discordance on flow dynamics at open channel confluences. *J. Hydraul. Eng.* 122 (12), 676–682.
- Blanchoud, H., Moreau-Guigon, E., Farrugia, F., Chevreuil, M., Mouchel, J.M., 2007. Contribution by urban and agricultural pesticide uses to water contamination at the scale of the Marne watershed. *Sci. Total Environ.* 375 (1-3), 168–179.
- Bruwier, M., Maravat, C., Mustafa, A., Teller, J., Pirotton, M., Ericum, S., Archambeau, P., Dewals, B., 2020. Influence of urban forms on surface flow in urban pluvial flooding. *J. Hydrol.* 582, 124493. <https://doi.org/10.1016/j.jhydrol.2019.124493>.
- Chang, S.E., 2016. Socioeconomic impacts of infrastructure disruptions. *Oxford Res Encyclopedia Natural Hazard Sci.* <https://doi.org/10.1093/acrefore/9780199389407.013.66>.
- Chang, T.J., Wang, C.H., Chen, A., Djordjevic, S., 2018. The effect of inclusion of inlets in dual drainage modelling. *J. Hydrol.* 559, 541–555. <https://doi.org/10.1016/j.jhydrol.2018.01.066>.
- Chen, A., Leandro, J., Djordjević, S., 2016. Modelling sewer discharge via displacement of manhole covers during flood events using 1D/2D SIPSON/P-D wave dual drainage simulations. *Urban Water J.* 13 (8), 830–840. <https://doi.org/10.1080/1573062X.2015.104199>.
- Chibane, T., Paquier, A., Benmamar, S., 2021. Experimental study of the flow patterns in a street during drainage or overflow to or from drains. *Urban Water J.* 18 (7), 544–557. <https://doi.org/10.1080/1573062X.2021.1913612>.
- Costabile, P., Costanzo, C., De Lorenzo, G., Macchione, F. Is local flood hazard assessment in urban areas significantly influenced by the physical complexity of the hydrodynamic inundation model? *Journal of Hydrology*, 580, 124231, doi:10.1016/j.jhydrol.2019.124231.

- de Man, H., van den Berg, H.H.J.L., Leenen, E.J.T.M., Schijven, J.F., van der Schets, F.M., Vliet, J.C., van Knapen, F., de Roda Husman, A.M., 2013. Quantitative assessment of infection risk from exposure to waterborne pathogens in urban floodwater. *Water Res.* 48 (1), 90–99.
- Deblonde, T., Cossu-Leguille, C., Hartemann, P., 2011. Emerging pollutants in wastewater: a review of the literature. *Int. J. Hyg. Environ. Health* 214 (6), 442–448.
- Defra, 2011, Annex B: National Build. Standards Design and Construction of New Gravity Foul Sewers and Lateral Drains Water Industry Act. 1991 Section 106B Flood and Water Management Act. 2010 Section 42 [online] available from <https://assets.publishing.service.gov.uk/government/uploads/system/uploads/attachment_data/file/82516/new-build-sewers-consult-annexb-sos-standards-111220.pdf> [25 October 2020].
- Del Giudice, F., Gisonni, C., Hager, W., 2000. Supercritical flow in 45° junction manhole. *J. Irrig. Drain. Eng.* 126 (1), 48–56.
- Djordjević, S., Prodanović, D., Maksimović, Č., Ivetić, M., Savić, D., 2005. SIPSON – simulation of interaction between pipe flow and surface overland flow in networks. *Water Sci. Technol.* 52 (5), 275–283.
- Djordjević, S., Saul, A.J., Tabor, G.R., Blanksby, J., Galambos, I., Sabtu, N., Sailor, G., 2013. Experimental and Numerical Investigation of Interactions between above and below Ground Drainage Systems. *Water Sci. Technol.* 67, 535–542. <https://doi.org/10.2166/wst.2012.570>.
- Fraga, I., Cea, L., Puertas, P., 2015. Validation of a 1D–2D dual drainage model under unsteady part-full and surcharged sewer conditions. *Urban Water J.* 14 (1), 74–84. <https://doi.org/10.1080/1573062X.2015.1057180>.
- Gallegos, Humberto A., Schubert, Jochen E., Sanders, Brett F., 2009. Two-dimensional, high-resolution modeling of urban dam-break flooding: a case study of Baldwin Hills, California. *Adv. Water Resour.* 32 (8), 1323–1335.
- Golian, Mohsen, Katibeh, Homayoon, Singh, Vijay P., Ostad-Ali-Askari, Kaveh, Rostami, Hamed Tavasoli, 2020. Prediction of tunnelling impact on flow rates of adjacent extraction water wells. *Eng. Geol. Hydrogeol.* 53 (2), 236–251. <https://doi.org/10.1144/qjehg2019-055>.
- Gómez, M., Russo, B., Tellez-Alvarez, J., 2019. Experimental Investigation to Estimate the Discharge Coefficient of a Grate Inlet under Surcharged Conditions. *Urban Water Journal* 16 (2), 85–91. doi:10.1080/1573062X.2019.1634107.
- Gómez, M., Hidalgo Rabassada, G., Russo, B., 2013. Experimental Campaign to Determine Grated Inlet Clogging Factors in an Urban Catchment of Barcelona. *Urban Water J.* 10 (1), 50–61. <https://doi.org/10.1080/1573062X.2012.690435>.
- Gómez, M., Recasens, J., Russo, B., Martínez-Gomariz, E., 2016. Assessment of Inlet Efficiency through a 3D simulation: numerical and experimental comparison. *Water Sci. Technol.* 74 (8), 1926–1935. <https://doi.org/10.2166/wst.2016.326>.
- Gotfredsen, E., Kunoy, J.D., Mayer, S., Meyer, K.E., 2020. Experimental validation of RANS and DES modelling of pipe flow mixing. *Heat Mass Transf.* 56, 2211–2224.
- Hammond, M.J., Chen, A.S., Djordjević, S., Butler, D., Mark, O., 2013. Urban flood impact assessment: a state-of-the-art review. *Urban Water J.* 12 (1), 14–29.
- Hofstra, Nynke, 2011. Quantifying the impact of climate change on enteric waterborne pathogen concentrations in surface water. *Curr. Opin. Environ. Sustain.* 3 (6), 471–479.
- Hou, Jingming, Han, Hao, Qi, Wenchao, Guo, Kaihua, Li, Zhanbin, Hinkelmann, Reinhard, 2019. Experimental investigation for impacts of rain storms and terrain slopes on low impact development effect in an idealized urban catchment. *J. Hydrol.* 579, 124176. <https://doi.org/10.1016/j.jhydrol.2019.124176>.
- Houston, D., Werrity, A., Bassett, D., Geddes, A., Hoolachan, A., and McMillan, M., 2011. *Pluvial (rain-related) flooding in urban areas: the invisible hazard* [online] available from <<http://eprints.gla.ac.uk/162145/7/162145.pdf>> [19 October 2020].
- Hsu, C.C., and Lee, J., 1998. Flow at 90° equal-width open channel junction. *Journal of Hydraulic Engineering*, 124, 186–191.
- Jang, J.H., Chan, T.H., Chen, W.B., 2018. Effect of inlet modelling on surface drainage in coupled urban flood simulation. *J. Hydrol.* 562, 168–180. <https://doi.org/10.1016/j.jhydrol.2018.05.010>.
- Kemper, S., and Schlenkhoff, A., 2019. Experimental Study on the Hydraulic Capacity of Grate Inlets with Supercritical Surface Flow Conditions. *Water Science and Technology* 79 (9), 1717–1726. doi:10.2166/wst.2019.171.
- Kesserwani, G., Seungsoo, L., Rubinato, M., Shucksmith, J., 2015. Experimental and numerical validation of shallow water flow around a surcharging manhole. Urban Drainage Modelling Conference, Mont-Sainte Anne Quebec, Canada.
- Kim, Sungpyo, Aga, Diana S., 2007. Potential ecological and human health impacts of antibiotics and antibiotic-resistant bacteria from wastewater treatment plants. *J. Toxicol. Environ. Health, Part B* 10 (8), 559–573.
- Lee, S., Nakagawa, H., Kawaike, K., Zhang, H., 2013. Experimental validation of interaction model at storm drain for development of integrated urban. *J. Jpn. Soc. Civil Eng., Ser. B* 1 (69), 109–114.
- Lee, S., Nakagawa, H., Kawaike, K., Zhang, H., 2015. Urban inundation simulation considering road network and building configurations. *J. Flood Risk Manage.* 9 (3), 224–233. <https://doi.org/10.1111/jfr3.12165>.
- Lopes, P., Shucksmith, J., Leandro, J., Fernandes de Carvalho, R., Rubinato, M., 2014. Velocities profiles and air-entrainment characterization in a scaled circular manhole, 2014, 13th ICUD, Sawarak, Malaysia.
- Lopes, P., Leandro, J., Carvalho, R.F., Páscoa, P., Martins, R., 2015. Numerical and experimental investigation of a gully under surcharge conditions. *Urban Water J.* 12 (6), 468–476. <https://doi.org/10.1080/1573062X.2013.831916>.
- Mark, O., Jørgensen, C., Hammond, M., Khan, D., Tjener, R., Erichsen, A., Helwigh, B., 2018. A new model of health risk from urban flooding. *J. Flood Risk Manage.* 11, S28–S42. <https://doi.org/10.1111/jfr3.12182>.
- Marsalek, J., Rochfort, Q., 2010. Urban wet-weather flows: sources of fecal contamination impacting on recreational waters and threatening drinking-water sources. *J. Toxicol. Environ. Health, Part A* 67 (20–22), 1765–1777.
- Martins, R., Leandro, J., Carvalho, R., 2014. Characterization of the hydraulic performance of a gully under drainage conditions. *Water Sci. Technol.* 69, 2423–2430. <https://doi.org/10.2166/wst.2014.168>.
- Martins, R., Kesserwani, G., Rubinato, M., Lee, S., Leandro, J., Djordjević, S., Shucksmith, J.D., 2017. Validation of 2D shock capturing flood models around a surcharging manhole. *Urban Water J.* 14 (9), 892–899.
- Martins, R., Rubinato, M., Kesserwani, G., Leandro, J., Djordjević, S., Shucksmith, J.D., 2018. On the characteristics of velocities fields in the vicinity of manhole inlet grates during flood events. *Water Resour. Res.* 54 (9), 6408–6422.
- Mignot, E., Li, X., Dewals, B., 2019. Experimental Modelling of Urban Flooding: A Review. *J. Hydrol.* 568, 334–342. <https://doi.org/10.1016/j.jhydrol.2018.11.001>.
- Mostafa, Simón, Rubinato, Matteo, Rosario-Ortiz, Fernando L., Linden, Karl G., 2016. Impact of light screening and photosensitization by surface water organic matter on enterococcus faecalis inactivation. *Environ. Eng. Sci.* 33 (6), 365–373.
- Naves, J., Anta, J., Suárez, J., Puertas, J., 2020. Hydraulic, wash-off and sediment transport experiments in a full-scale urban drainage physical model. *Sci. Data* 7 (1), 44. <https://doi.org/10.1038/s41597-020-0384-z>.
- Nichols, A., Rubinato, M., 2016. Remote sensing of environmental processes via low-cost 3D free-surface mapping. IHAR Europe Congress, Liege, Belgium.
- Noh, Seong Jin, Lee, Seungsoo, An, Hyunuk, Kawaike, Kenji, Nakagawa, Hajime, 2016. Ensemble urban flood simulation in comparison with laboratory-scale experiments: impact of interaction models for manhole, sewer pipe, and surface flow. *Adv. Water Resour.* 97, 25–37. <https://doi.org/10.1016/j.adwatres.2016.08.015>.
- Ofwat, 2011, Future Impacts on Sewer Systems in England and Wales [online] available from <https://www.ofwat.gov.uk/wp-content/uploads/2015/11/rpt_com201106mottmacsewer.pdf> [19 October 2020].
- Ostad-Ali-Askari, Kaveh, Ghorbanizadeh Khazari, Hossein, Shayannejad, Mohammad, Zareian, Mohammad Javad, 2019. Effect of management strategies on reducing negative impacts of climate change on water resources of the Isfahan-Borkhar aquifer using MODFLOW. *River Res. Appl.* 35 (6), 611–631. <https://doi.org/10.1002/rra.v35.610.1002/rra.3463>.
- Pfister, Michael, Gisonni, Corrado, 2014. Head losses in junction manholes for free surface flows in circular conduits. *J. Hydraulic Eng.* 140 (9), 06014015. [https://doi.org/10.1061/\(ASCE\)HY.1943-7900.0000895](https://doi.org/10.1061/(ASCE)HY.1943-7900.0000895).
- Ramamurthy, Amruthur S., Carballada, Luis B., Tran, Due Minn, 1988. Combining open channel flow at right angled junctions. *J. Hydraul. Eng.* 114 (12), 1449–1460.
- Ramamurthy, A.S., Zhu, Weimin, 1997. Combining flows in 90 junctions of rectangular closed conduits. *J. Hydraul. Eng.* 123 (11), 1012–1019.
- Rojas Arques, Santiago, Rubinato, Matteo, Nichols, Andrew, Shucksmith, James D., 2018. Cost effective measuring technique to simultaneously quantify 2D velocity fields and depth-averaged solute concentrations in shallow water flows. *J. Flow Meas. Instrum.* 64, 213–223.
- Rossi, Luca, de Alencastro, Luiz, Kupper, Thomas, Tarradellas, Joseph, 2004. Urban stormwater contamination by polychlorinated biphenyls (PCBs) and its importance for urban water systems in Switzerland. *Sci. Total Environ.* 322 (1–3), 179–189.
- Rubinato, M., 2015. Physical Scale Modelling of Urban Flood Systems. PhD Thesis. The University of Sheffield.
- Rubinato, M., Lashford, C., Goerke, M. (2020b) Chapter 9: Advances in experimental modelling of urban flooding, *IWA Publishing 2021. Water-Wise Cities and Sustainable Water Systems: Concepts, Technologies, and Applications*, doi:10.2166/9781789060768_0235.
- Rubinato, M., Martins, R., Kesserwani, G., Leandro, J., Djordjević, S., Shucksmith, J., 2017. Experimental calibration and validation of sewer/surface flow exchange equations in steady and unsteady flow conditions. *J. Hydrol.* 552 (1), 421–432.
- Rubinato, M., Lee, S., Martins, R., Shucksmith, J.D., 2018a. Surface to sewer flow exchange through circular inlets during urban flood conditions. *J. Hydroinf.* 20 (3), 564–576.
- Rubinato, M., Martins, R., Shucksmith, J.D., 2018b. Quantification of energy losses at a surcharging manhole. *Urban Water J.* 15 (3), 234–241.
- Rubinato, M., Luo, M., Zheng, X., Pu, J.H., Shao, S., 2020a. Advances in modelling and prediction on the impact of human activities and extreme events on environments. *Water* 12 (6), 1768. <https://doi.org/10.3390/w12061768>.
- Rubinato, Matteo, Nichols, Andrew, Peng, Yong, Zhang, Jian-min, Lashford, Craig, Cai, Yan-peng, Lin, Peng-zhi, Tait, Simon, 2019. Urban and river flooding: comparison of flood risk management approaches in the UK and China and an assessment of future knowledge needs. *Water Sci. Eng.* 12 (4), 274–283.
- Rubinato, M., Shucksmith, J., Saul, A.J., Shepherd, W., 2013. Comparison between InfoWorks results and a physical model of an urban drainage system. *Water Sci. Technol.* 68 (2), 372–379. <http://wst.iwaponline.com/content/68/2/372>.
- Rutherford, J.C., 1994. *River Mixing*. J. Wiley & Sons, New York, p. 336.
- Saldarriaga, J., Rincon, G., Moscote, G., Trujillo, M., 2017. Symmetric junction manholes under supercritical flow conditions. *J. Hydraul. Res.* 55 (1), 135–142. <https://doi.org/10.1080/00221686.2016.1212410>.
- Sales-Ortells, Helena, Agostini, Giulia, Medema, Gertjan, 2015. Quantification of waterborne pathogens and associated health risks in urban water. *Environ. Sci. Technol.* 49 (11), 6943–6952.
- Schets, F.M., van Wijnen, J.H., Schijven, J.F., Schoon, H., de Roda Husman, A.M., 2008. Monitoring of Waterborne Pathogens in Surface Waters in Amsterdam, The Netherlands, and the Potential Health Risk Associated with Exposure to Cryptosporidium and Giardia in These Waters. *Appl. Environ. Microbiol.* 74 (7), 2069–2078.
- Shucksmith, J., Rubinato, M., Martins, R., Kesserwani, G., Leandro, J., Djordjević, S., Understanding pollutant transport in urban floodwater for health impact assessment

- using a physical scale model , 23-26 September 2018, 11th International Conference on Urban Drainage Modelling, Palermo, Italy.
- Swan, Andrew, 2010. How increased urbanisation has induced flooding problems in the UK: A lesson for African cities? *Phys. Chem. Earth, Parts A/B/C* 35 (13-14), 643–647.
- Taylor, G., 1954. The dispersion of matter in turbulent flow through a pipe. *Proc. R. Soc. Lond. A* 223, 446–468. <https://doi.org/10.1098/rspa.1954.0130>.
- Tellez-Alvarez, J., Gómez, M., Russo, B., 2020. Quantification of energy loss in two grated inlets under pressure. *Water* 12 (6), 1601. <https://doi.org/10.3390/w12061601>.
- Zevenbergen, C., Veerbeek, W., Gersonius, B., Van Herk, S., 2008. Challenges in urban flood management: travelling across spatial and temporal scales. *J. Flood Risk Manage.* 1 (2), 81–88.
- Zhao, Can-Hua, Zhu, David Z., Rajaratnam, Nallamuthu, 2006. Experimental study of surcharged flow at combining sewer junctions. *J. Hydraul. Eng.* 132 (12), 1259–1271.
- Zhao, Can-Hua, Zhu, David Z., Rajaratnam, Nallamuthu, 2008. Computational and Experimental Study of Surcharged Flow at a 90 Combining Sewer Junction. *J. Hydraul. Eng.* 134 (6), 688–700.